AJAPAS

# African Journal of Advanced Pure and Applied Sciences (AJAPAS)

*Online ISSN: 2957-644X*

Volume 3, Issue 3, 2024, Page No: 25-37

Website: *https://aaasjournals.com/index.php/ajapas/index*

معامل التأثير العربي 2023: (1.55) SJIFactor 2023: 5.689 ISI 2022-2023: 0.557

**Special issue: First Libyan Conference on Technology and Innovation (LCTI-2024), Benghazi, Libya**

# التنبؤ بالمكامن الجيوحرارية وإمكانية توليد الطاقة باستخدام خصائص الماء المُنتج في الحقول النفطية

إبراهيم محمد أبو الليل[1]، سهام نجيب توفيق[2*]، عبد المنعم حسن[3]
[1] قسم الهندسة النفطية، كلية الهندسة، جامعة طبرق، طبرق، ليبيا
[2] قسم الهندسة الكيميائية، كلية الهندسة، جامعة طبرق، طبرق، ليبيا
[3] قسم الطاقات المتجددة، أكاديمية الدراسات العليا، طبرق، ليبيا

# Reservoirs Geothermal Prediction and Potentiality of Power Generation Utilizing Brine Characterizations Produced in Oil Fields

Ibrahim M. Abou El Leil[1], Seham N. Tawfic[2*], Abdel Moneam Hassn[3]
[1]Petroleum Engineering Department, Faculty of Engineering, Tobruk University, Tobruk, Libya
[2]Chemistry Engineering Department, Faculty of Engineering, Tobruk University, Tobruk, Libya
[3]Renewable Energy Department, Higher Studies Academy, Tobruk, Libya

[*]Corresponding author: seham67@hotmail.com

| Received: March 01, 2024 | Accepted: May 05, 2024 | Published: May 30, 2024 |
| --- | --- | --- |

**الملخص**

الطاقة الجيوحرارية (طاقة الحرارة الأرضية) هي طاقة حرارية تتشكل بشكل طبيعي تحت سطح الأرض. كما أنها تُعدُ واحدةً من المصادر الهامة للطاقات المتجددة، ومن المتوقع أن تكون قادرة على إنتاج الطاقة الكهربائية كبديل للوقود الأحفوري في المستقبل. ويعتبر البحث في درجة حرارة المكامن من البحوث الأساسية لاستكشاف أصل الموائع وتقدير درجة حرارة المكامن بهدف تحديد المصادر المحتملة للطاقة الجيوحرارية من الظواهر السطحية. وتهدف هذه الدراسة إلى إبراز إمكانية استخدام التوصيفات الكيميائية مثل تركيزات الكاتيونات في المياه المُنتَجة (الماء الأُجاج) في آبار النفط للتنبؤ بدرجة حرارة المكمن، وذلك لأن درجة حرارة الماء تُعدُ أحد العوامل الرئيسية لتعيين وتصنيف المكمن الجيوحراري مثل المكامن منخفضة الإنثالبي، متوسطة الإنثالبي وعالية الإنثالبي. كما يُعد استخدام الطاقة الجيوحرارية لتوليد الطاقة الكهربائية أحد الاستخدامات الرئيسية كمصدر للطاقة، وذلك باستخدام ثلاثة أنواع أساسية من محطات الطاقة الجيوحرارية: البخار الجاف، البخار الوميضي، والمزدوج. لقد تم اختيار اثنى عشر بئراً نفطياً في حقل جالو بمنطقة الواحات في الجنوب الليبي لدراسة تقدير درجة حرارة المكمن الجيوحراري من الدلائل التي تمت باستخدام معادلات مقياس الحرارة لحساب درجة الحرارة التي اشتملت على تركيزات كاتيونات $Na^{+}$ ، $K^{+}$، $Ca^{++}$، و $SiO_2$ ، وقد أظهرت النتائج المتحصل أن التصنيف الجيوحراري للمكمن طبقاً للمصادر المنشورة لتقسيم الانثالبي فقد تم تقسيمها إلى منخفضة جداً، منخفضة، متوسطة وعالية. وبناءً على هذا التقسيم فإن إمكانية توليد الطاقة الكهربائية تتباين طبقاً للقيم الجيوحرارية ومن ثمَ نظم المحطات الكهربائية. وبشكلٍ عام يمكن في الوقت الحالي وباستخدام التكنولوجيا الحالية تطبيقها في محطات توليد الطاقة الكهربائية التي تعتمد على الطاقة الجيوحرارية. كما يمكن تطبيقها في الاستخدامات المباشرة وغير المباشرة.

**الكلمات المفتاحية:** طاقة جيوحرارية، طاقة متجددة، مكمن، درجة حرارة، ماء مُنتج، المواصفات الكيميائية، توليد الطاقة.

**Abstract**

Geothermal is heat energy that is naturally formed below the ground surface. It is one of the important source of renewable energies which is expected to be able to produce electrical power as an alternative of fossil fuels in the future. Reservoir temperature research is fundamental initial research to explore the origin of fluids and reservoir temperature estimation to determine the potential sources of geothermal from surface manifestations. This study is aiming highlights the potentiality of utilization the chemical characterizations such as cations concentrations in produced water (Brine) in oil wells to predict reservoir temperature because of the degree of water temperature is main parameter to determine and classify the geothermal reservoir e.g. law, medium or high enthalpy. Whereas, one of the key uses of geothermal energy is electric-power generation using three basic types of geothermal power plants: *dry steam*, *flash steam*, and *binary*. Twelve producing oil wells in Jailo oilfield were selected for temperature estimation study of the geothermal reservoir has been carried out using geothermometer equations for temperature calculations involving the concentrations of $Na^+$, $K^+$, $Ca^{++}$, and $SiO_2$. The obtained results revealed that the geothermal classification of reservoirs according to the published references using enthalpy type there are a different enthalpies and the geothermal of reservoir can be classified into Ultra low enthalpy, very low enthalpy, medium enthalpy and high enthalpy. Consequently of these classification the potentiality of electric power generation varies according the geothermal temperature degree and the power plant system. Generally it could be in the current time and with the application of current technology, geothermal energy generator electricity power plant can be applied and the geothermal temperature can be applied for direct and indirect geothermal applications.

**Keywords:** Geothermal, renewable energy, reservoir, temperature, produced water, chemical characterizations, power generation.

## 1. Introduction

### 1.1. Geothermal Energy

The term "geothermal" means "Earth heat" or "heat of the Earth". Energy from geothermal resources has benefited humankind from its earliest origins. Prehistoric civilizations used hot springs and steam discharges (fumaroles) for cooking, heating, and therapeutic bathing; in modern terms, these uses are known as geothermal direct-use applications. In the United States, geothermal energy has provided affordable, reliable, and renewable energy since the 1890s, when the city of Boise, Idaho, began using geothermal resources for direct heating of commercial and residential buildings (Milliken, 2017). Since then, use of geothermal energy in the United States has expanded to include utility-scale electricity production, distributed heating and cooling applications, and the augmentation of various industrial processes.

Geothermal energy is a renewable and alternative source of energy extracted from the heat stored below Earth's surface (Aliyu, et al., 2019; Feng, et al., 2020; Avci, et al., 2020). Below Earth's crust, a magmatic layer generates heat because of the continuous decay of radioactive materials such as uranium, thorium, and potassium (Nelson, 2017; Barbier, 202; Ikshvaku, et al., 2018). Heat is transported to the surface because of the crustal movement, caused by convective heat transfer (Avci, et al., 2020; Santamaria, 2020), where high-temperature and -pressure conditions cause plastic behavior in the rocks in Earth's mantle. Density differences lead to lighter and hotter portions of the mantle to move upward, heating rocks and water present in Earth's crust to temperatures of >370 °C (Nelson, 2017). Conduction is the primary heat transfer mechanism in Earth's crust (Morgan, 1984) caused by interactions between lithospheric plates (Santamaria, 2020). Earth's geothermal energy will last for 4–5 billion years, and that heat stored in 10 km of Earth's surface holds heat equivalent to 50,000 times more energy than all of the world's oil and gas reserves (Nelson, 2017). On a yearly basis, 10,000,000 GWh of heat is conducted from Earth's interior to the surface (Avci, et al., 2020).

### 1.1.2. Geothermal Classification

Younger (2015) gives a proposal for the categorization of geothermal resources according to their pressure, temperature and enthalpy, as shown in Figure 1. The enthalpy is a property of a thermodynamic system and is equal to the internal energy of the system plus the product of its pressure and volume.

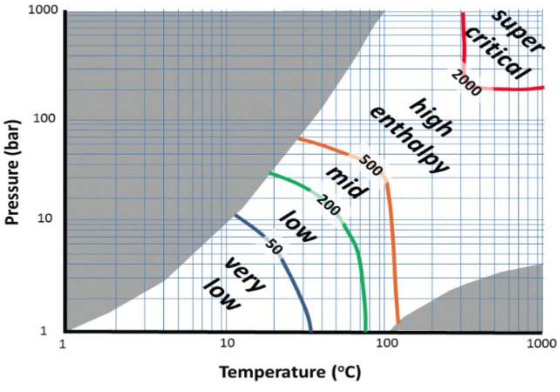


**Figure 1:** Geothermal resources classification (Younger, 2015).

Geothermal resources may be classified as low, medium, or high enthalpy based on the geothermal resource temperature and thermodynamic properties. The United States Geological Survey (USGS) establishes the boundaries between low, medium and high enthalpy resources as <90 °C, between 90 and 150 °C and >150 °C, respectively (Williams, et al., 2011). Moreover, Figure 2 shows the alternative classifications proposed by other authors for which the criteria for each type of geothermal resource vary per the temperature.

Medium- and low-enthalpy fluids can generate electricity by installing binary cycle power plants. A binary cycle power plant comprises an evaporator, expander, pump, condenser, and heat source (Tchanche, et al., 2013). Countries, such as Germany (Eyerer, et al., 2021; Baujard, et al., 2018; Watanabe, et al., 2017), the United States (Holdmann, 2007; DiPippo, et al., 2013), Indonesia (Frick, et al., 2019), (46) Austria (Pernecker and Uhlig, 2002; Legmann, 2003), and Portugal (Rangel, et al., 2017), have used the organic Rankine cycle (ORC), a form of binary cycle power generation technology, which is the primary mechanism for electrical production from geothermal resources. The working principle of the ORC is similar to that of the conventional Rankine cycle. However, rather than water, the working fluid is an organic fluid with a higher molecular mass and a lower boiling point than that of water (Mahmoudi, et al., 2018; Ahmadi, et al., 2020).

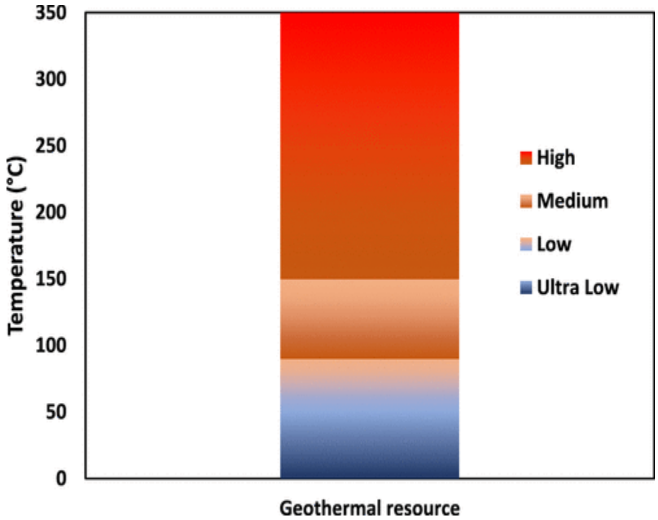


**Figure 2:** Classification of geothermal resources based on temperature. Color scale from blue (ultralow enthalpy geothermal resource) to red (high enthalpy geothermal resource) (Williams, et al., 2011)

### 1.1.3. Hydrothermal Resources

Naturally occurring hydrothermal resources contain the basic elements of heat in the Earth, along with groundwater and rock characteristics (i.e., open fractures that allow fluid flow) sufficient for the recovery of heat energy, usually through produced hot water or steam. Hydrothermal resources can range in temperature from a few degrees above ambient conditions to temperatures greater than 375°C. Above this higher range, a new class of innovative subsurface and surface production technologies will likely be required to convert geothermal energy resources for beneficial use.

## 2. Produced Water In Oilfeilds

Water produced during oil and gas extraction operations may be called formation water, oilfield water and brine, and constitutes the industry’s most important waste stream on the basis of volume. Today, nearly 115 billion barrels per year (bbl/y) of water are produced worldwide as a by-product of oil and gas (Veil, et al., 2004). In average, for every barrel of oil, three barrels of water are produced from oil wells.

### 2.1. Definition of Produced Water

Produced water is water found in the same formations as oil and gas. When the oil and gas are produced to the surface, the produced water is brought to the surface, too. It is also referred to as “brine,” “saltwater,” or “formation water.” Produced water contains some of the chemical characteristics of the formation from which it was produced and associated hydrocarbons.

### 2.2. Chemical Composition

Because of long-time contact with the reservoir rocks and crude oil, the formation water contains a considerable deal of metallic salts, such as sodium salt, potassium salt, calcium salt, and magnesium salt, and for this reason, the formation water is also called brine. Formation water has competitively higher salt concentration that makes the formation water distinguished from the land-surface water. The total salt concentration in formation water is called salinity.

Positive ions commonly encountered in formation water include $Na^+$, $K^+$, $Ca^{2+}$, and $Mg^{2+}$, and some other positive ions such as $Ba^{2+}$, $Fe^{2+}$, $Sr^{2+}$, and Li+ also take a little share; the commonly encountered negative ions include $C1^-$, $SO4^{2-}$, $HCO_3^{-}$, $CO3^{2-}$, $NO_3$, and $Br^-$, as well as some trace ions.

**3. Location Of Study**

Jailo oilfield was located in the south of Libya at Oasis area (Figure 3). This study was carried out on the produced water of Gailo oilfield for oil producing wells to distinguish the characterizations of the water production. Also, the water characteristics.

**4. Study Objectives**

The objectives of this study are as following:

(1) Describe the characteristics of produced water: constituent concentration.
(2) Identify potential beneficial uses of produced water.
(3) Identify constituents in produced water that exceed water quality requirements of beneficial uses.
(4) Geothermal classification.
(5) The potentiality of utilization of this water for electricity generation.

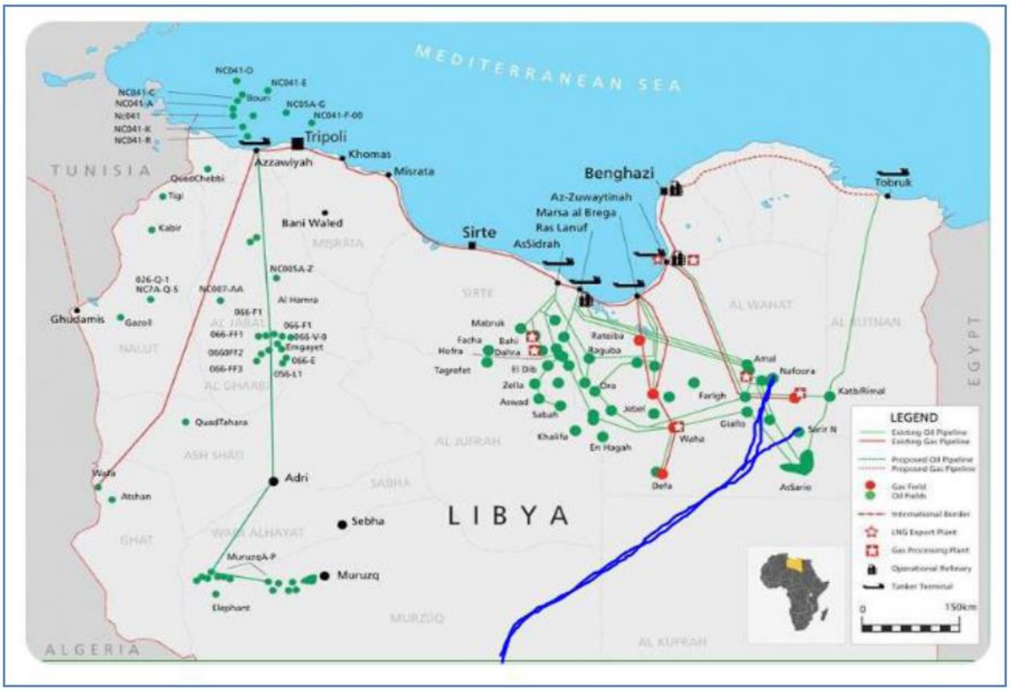


**Figure 3:** A map showing wells locations of Sarir and Nafora oilfields (APICORP, 2018).

**5. Methodology**

This study utilized several water samples in the hot water manifestation of Nafora oil field with 10 different oil wells of hot water because the wells is the biggest source. At each well, the temperature of hot water is measure, and pH is measure by a pH meter. Also, the water samples were analyzed using the Atomic Absorption Spectrophotometer (AAS) method of Na, K, and $SiO_2$ content for each water sample. From the results of the analysis by using the methods, Na-K, $SiO_2$, and Na-K-Ca calculations were performed to predict reservoir temperature by using the following Equations (DiPippo, 2012):

$$T = \frac{1217}{log_{10}\frac{(Na)}{(K)}+1.483} - 273.15 \quad (1)$$

$$T = \frac{1647}{log_{10}\frac{(Na)}{(K)}+\beta\left[log_{10}\frac{\sqrt{(Ca)}}{(Na)}+2.06\right]} - 273.15 \quad (2)$$

$$T = \frac{1309}{5.19 - log_{10}(Si)} - 273.15 \quad (3)$$

where:

$Na$ : sodium concentration

$K$ : potassium concentration

$Ca$ : calcium concentration

$Si$ : concentration of silicon

$\beta = 4/3$, if $T < 100$ ◦C

$\beta = 1/3$, if $T > 100$ ◦C

## 6. RESULTS AND DISCUSSION

### 6.1. Water Characteristics

The investigated water samples of twelve producing wells namely GialoW1 to GialoW12 under consideration have been analyzed to determine their constituents for some cations, silicon oxide and pH values, and the results are presented in Table 1.

**Table 1:** Chemical constituents of produced water.

| No | Produced Water Wells | Water Constituents | | | | |
|---|---|---|---|---|---|---|
| | | Cations Concentration (mg/l) | | | | |
| | | pH | $Na^+$ | $K^+$ | $Ca^{++}$ | $SiO_2$ |
| 1 | GialoW1 | 6.27 | 14718.34 | 390.50 | 1810.28 | 4.22 |
| 2 | GialoW2 | 6.56 | 7715.50 | 260.12 | 722.90 | 5.16 |
| 3 | GialoW3 | 6.48 | 7916.30 | 180.10 | 695.80 | 4.99 |
| 4 | GialoW4 | 6.30 | 8030.55 | 201.15 | 794.10 | 4.89 |
| 5 | GialoW5 | 5.94 | 8250.70 | 205.14 | 849.12 | 5.20 |
| 6 | GialoW6 | 6.80 | 14268.0 | 376.40 | 1740.10 | 5.88 |
| 7 | GialoW7 | 6.79 | 7998.60 | 235.44 | 634.09 | 6.19 |
| 8 | GialoW8 | 6.74 | 10310.90 | 295.11 | 1123.14 | 5.79 |
| 9 | GialoW9 | 6.91 | 10940.50 | 296.16 | 1063.18 | 4.32 |
| 10 | GialoW10 | 5.99 | 12366.25 | 320.10 | 1246.17 | 3.99 |
| 11 | GialoW11 | 6.45 | 14500.20 | 195.44 | 1040.90 | 4.98 |
| 12 | GialoW12 | 6.65 | 12621.32 | 218.40 | 915.88 | 3.86 |
| Range | | 5.94-6.91 | 8030.55-14718.34 | 180.10-390.50 | 634.09-1810.28 | 3.86-6.19 |
| Average ($\bar{x}$) | | 6.49 | 10803.10 | 264.51 | 1052.97 | 4.82 |

On other hand, the obtained results are represented graphically throughout the bar charts to distinguish the range of variation of these constituents through the different producing wells. It is obviously from Figures 4 through 8 a wide variation of the studied parameters e. g. pH, $Na^+$, $K^+$, $Ca^{++}$ and $SiO_2$. This differences of produced water from well to another attributed to the chemical composition of the water. From Table 1 the measurement result of pH is between (5.94-6.91) with an average values of 6.49 (pH = 7). It indicated that the hot water in producing wells have a neutral pH.

As a result, the produced water is deserved to use for the research of modeling and estimating geothermal reservoir (Maryanto, et al., 2017). The results of the contents of Na, K, Ca and $SiO_2$ in each water sample shown in Table 1.

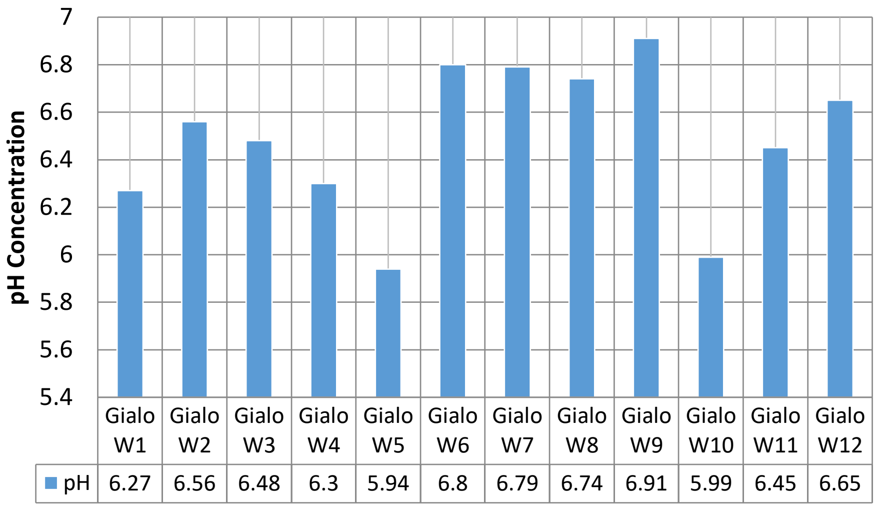


**Figure 4:** pH distribution in the exanimated water samples.

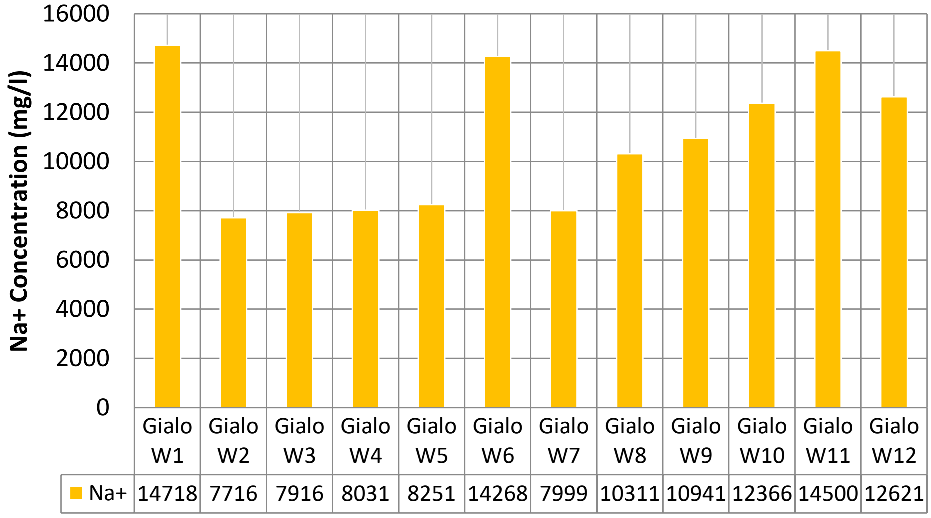


**Figure 5:** Sodium cation concentration in the water samples.

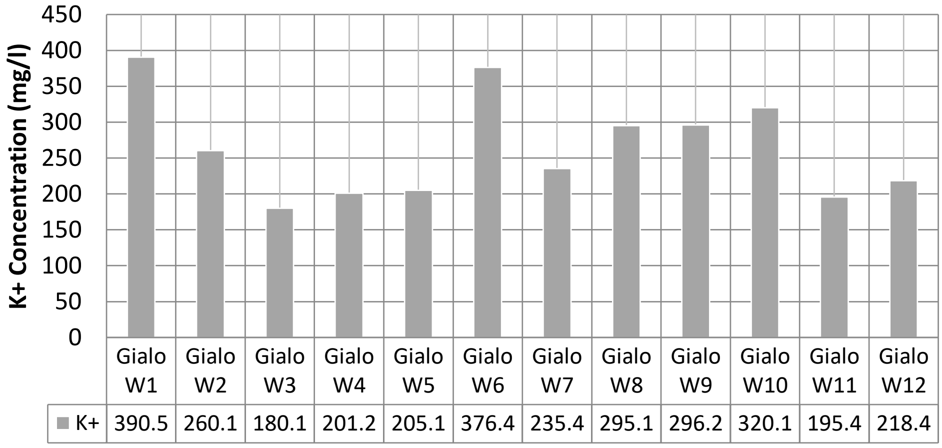


**Figure 6:** Potassium cation concentration in the water samples.

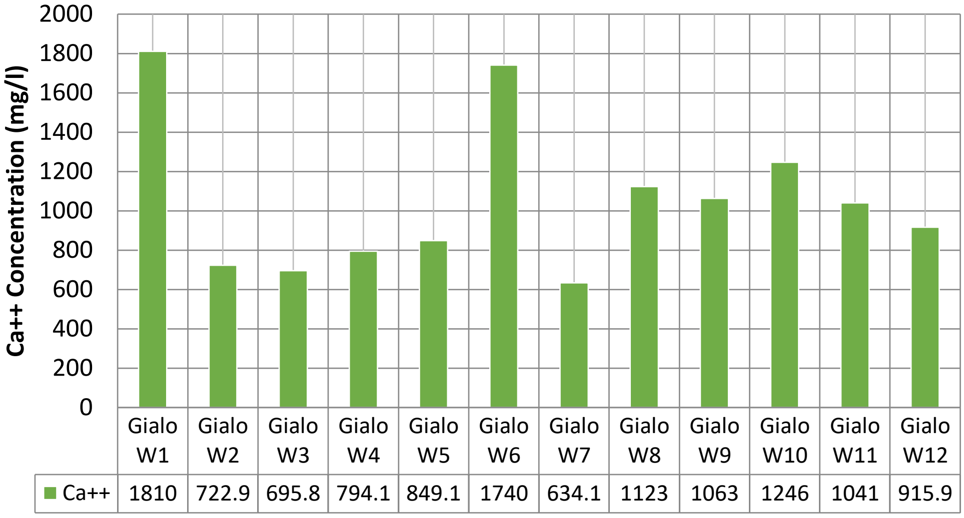


**Figure 7:** Calcium cation concentration in the water samples

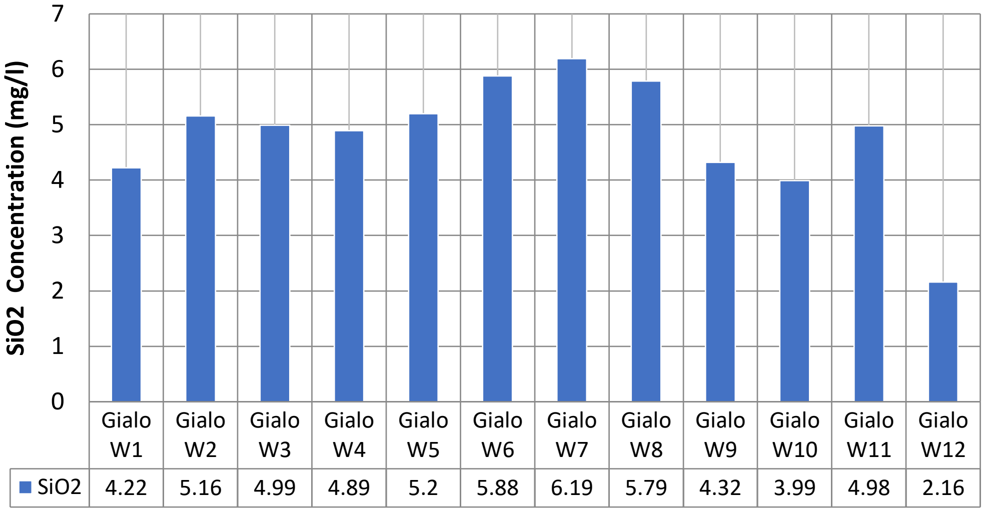


**Figure 8:** Silicon oxide content in the water samples

### 6.2. Calculation Methods

#### 6.2.1. Cations $Na^+$-$K^+$ Method Calculations

The reservoir temperature can be estimated using both sodium and potassium cations content (Idroes, *et al.*, 2019) by applying Equation [1] and the obtained results are presented in Table 2.

From Na and K contents showed that geothermal temperature estimation is the same as the data in Table 2. The lowest reservoir temperature is 89.77ºC, and the highest reservoir temperature is 138.67ºC, while the average temperature is 120.55ºC. Na-K geothermometer method is appropriate to predict geothermal reservoir temperature. Rock formation arrangement positively influences the geothermal reservoir so that the reservoir temperature results of Na-K (Table 2) can be used as a source of heat for power generation.

**Table 2:** The results of $Na^+$-$K^+$ cations method calculations.

| No | Produced Water Wells | Concentration (mg/l) | | Geothermal Temperature Estimation (T ºC) | Geothermal Temperature Estimation (T ºF) |
|---|---|---|---|---|---|
| | | $Na^+$ | $K^+$ | | |
| 1 | GialoW1 | 14718.34 | 390.50 | 124.66 | 256.39 |
| 2 | GialoW2 | 7715.50 | 260.12 | 138.67 | 281.61 |
| 3 | GialoW3 | 7916.30 | 180.10 | 116.16 | 241.09 |
| 4 | GialoW4 | 8030.55 | 201.15 | 121.44 | 250.59 |
| 5 | GialoW5 | 8250.70 | 205.14 | 121.03 | 249.85 |

| | | | | | |
|---|---|---|---|---|---|
| 6 | GialoW6 | 14268.00 | 376.40 | 124.34 | 255.81 |
| 7 | GialoW7 | 7998.60 | 235.44 | 130.61 | 267.10 |
| 8 | GialoW8 | 10310.90 | 295.11 | 128.99 | 264.18 |
| 9 | GialoW9 | 10940.50 | 296.16 | 125.80 | 258.44 |
| 10 | GialoW10 | 12366.25 | 320.10 | 123.27 | 253.89 |
| 11 | GialoW11 | 14500.20 | 195.44 | 89.77 | 193.59 |
| 12 | GialoW12 | 12621.32 | 218.40 | 101.91 | 215.44 |
| Range | | 8030.55-14718.34 | 180.10-390.50 | 89.77-138.67 | 215.44-281.61 |
| Average ($\bar{x}$) | | 10803.10 | 264.51 | 120.55 | 248.99 |

Figure 9 illustrates the variation of water temperature of the investigated wells, whereas the highest value was recorded in GialoW2 while the lowest one is recorded in GialoW11.

### 6.2.2. Cations $Na^{+}$-$K^{+}$-$Ca^{++}$ Method Calculations

The equilibrium between feldspar Na & K, calcite, or mineral containing Ca and hot water is described on geothermometer Na-K-Ca. It applies hot water having high Ca content (Giggenbach, 1988). From the laboratory analysis of Na-K-Ca and Equation [2], it is obtained the geothermal temperature estimation that presented in Table 3. The lowest temperature estimation is 711.42°C in GialoW11 and the highest temperature is 956.34°C in GialoW2with an average is 860.41°C. The bar charts of Figure 10 depicts the variance of geothermal temperature for the investigated wells.

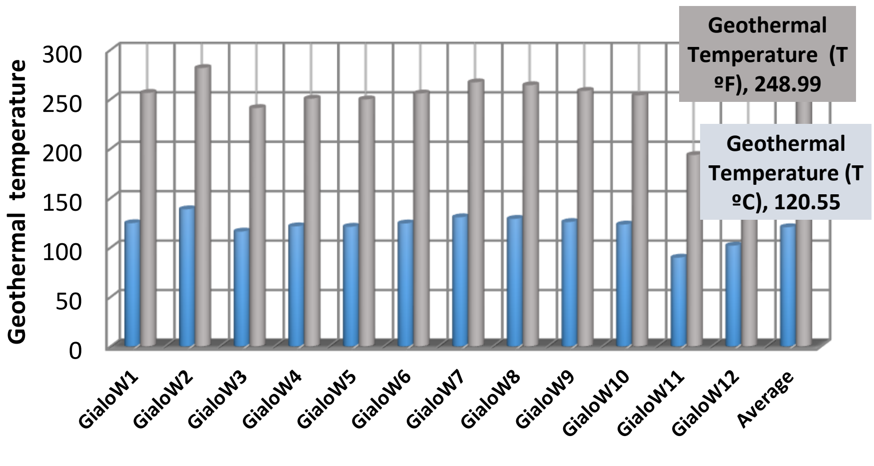


**Figure 9:** $Na^{+}$-$K^{+}$- geothermal temperature estimation.

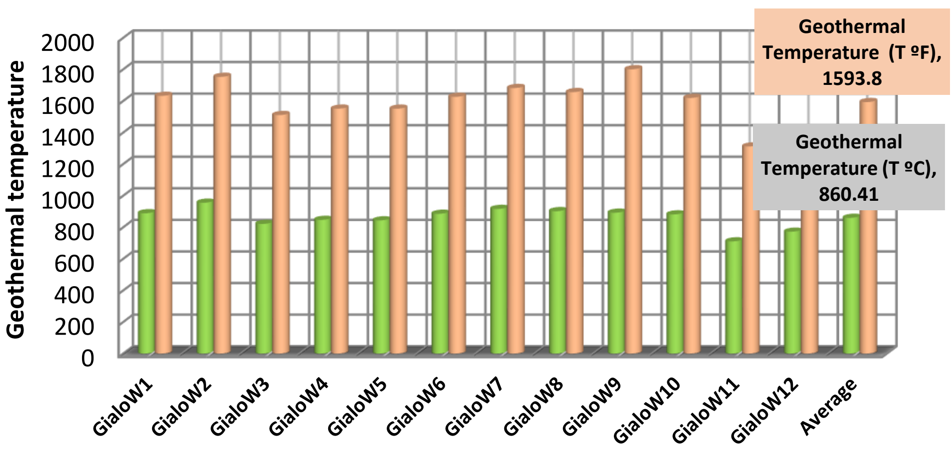


**Figure 10:** $Na^{+}$-$K^{+}$-$Ca^{++}$ geothermal temperature estimation.

**Table 3:** The results of $Na^+$-$K^+$-$Ca^{++}$ cations method calculations

| No | Produced Water Wells | Concentration (mg/l) | | | Geothermal Temperature Estimation (T ºC) | Geothermal Temperature Estimation (T ºF) |
|---|---|---|---|---|---|---|
| | | $Na^+$ | $K^+$ | $Ca^{++}$ | | |
| 1 | GialoW1 | 14718.34 | 390.50 | 1810.28 | 889.51 | 1633.12 |
| 2 | GialoW2 | 7715.50 | 260.12 | 722.90 | 956.34 | 1753.41 |
| 3 | GialoW3 | 7916.30 | 180.10 | 695.80 | 821.99 | 1511.58 |
| 4 | GialoW4 | 8030.55 | 201.15 | 794.10 | 847.54 | 1552.17 |
| 5 | GialoW5 | 8250.70 | 205.14 | 849.12 | 844.39 | 1551.90 |
| 6 | GialoW6 | 14268.0 | 376.40 | 1740.10 | 886.15 | 1627.07 |
| 7 | GialoW7 | 7998.60 | 235.44 | 634.09 | 917.03 | 1682.65 |
| 8 | GialoW8 | 10310.90 | 295.11 | 1123.14 | 902.76 | 1656.97 |
| 9 | GialoW9 | 10940.50 | 296.16 | 1063.18 | 893.06 | 1801.51 |
| 10 | GialoW10 | 12366.25 | 320.10 | 1246.17 | 882.26 | 1620.07 |
| 11 | GialoW11 | 14500.20 | 195.44 | 1040.90 | 711.42 | 1312.56 |
| 12 | GialoW12 | 12621.32 | 218.40 | 915.88 | 772.48 | 1422.64 |
| Range | | 8030.55-14718.34 | 180.10-390.50 | 634.09-1810.28 | 711.42-956.34 | 1312.56-1753.41 |
| Average ($\bar{x}$) | | 10803.10 | 264.51 | 1052.97 | 860.41 | 1593.80 |

**6.2.3. Silicon Oxide ($SiO_2$) Method Calculations**

After the analysis results of the Na-K geothermometer method, the analysis using the silica geothermometer ($SiO_2$) method was then carried out. From the concentration mg/l contents (Table 4) and the use of calculation in Equation [3] we can get the geothermal temperature degrees:

The obtained values of temperature reveal that the highest geothermal temperature estimation is 24.46ºC, which is located in GialoW7, and the lowest temperature is 11.20ºC for GialoW12 (Table 4). Meanwhile, the average temperature is 64.09ºC. The data are represented graphically as shown in Figure 11.

From those results, it cannot be used either to predict reservoir temperature because it is under surface hot water temperature. Where the deeper it gets, the higher the temperature obtained. According to Zheng and Zhang (2010), temperature increase indicates more or less 3ºC/100 m.

**Table 4:** The results of $SiO_2$ method calculations.

| No | Produced Water Wells | Concentration (mg/l) | Geothermal Temperature Estimation (T ºC) | Geothermal Temperature Estimation (T ºF) |
|---|---|---|---|---|
| | | $SiO_2$ | | |
| 1 | GialoW1 | 4.22 | 13.62 | 56.52 |
| 2 | GialoW2 | 5.16 | 19.21 | 66.58 |
| 3 | GialoW3 | 4.99 | 18.26 | 64.87 |
| 4 | GialoW4 | 4.89 | 17.69 | 63.84 |
| 5 | GialoW5 | 5.20 | 19.43 | 66.97 |
| 6 | GialoW6 | 5.88 | 22.96 | 73.33 |
| 7 | GialoW7 | 6.19 | 24.46 | 76.03 |
| 8 | GialoW8 | 5.79 | 22.51 | 72.52 |
| 9 | GialoW9 | 4.32 | 14.26 | 57.67 |
| 10 | GialoW10 | 3.99 | 12.10 | 53.78 |
| 11 | GialoW11 | 4.98 | 18.21 | 64.78 |
| 12 | GialoW12 | 3.86 | 11.20 | 52.16 |
| Range | | 3.86-6.19 | 11.20-24.46 | 52.16-76.03 |
| Average ($\bar{x}$) | | 4.82 | 17.83 | 64.09 |

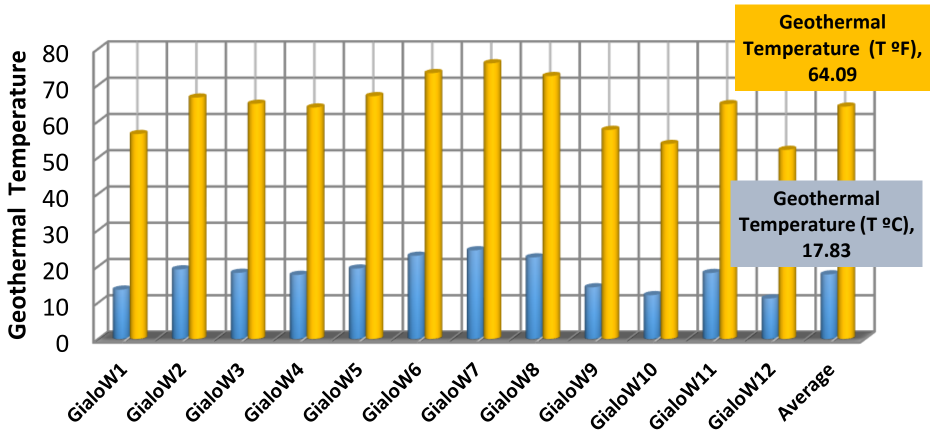


**Figure 11:** $SiO_2$ geothermal temperature estimation.

## 7. Geothermal Temperature Classification

Geothermal resources can be sorted into low, intermediate and high enthalpy sources according to the average reservoir temperature (Table 5). The classes of resources depicted in Table 5 are divided subjectively according to different authors. The authors cited do not reach a consensus on the appropriate temperature ranges to describe each class of geothermal resource. In the case of a closed loop geothermal system the corrected bottomhole temperature of the borehole is a good estimate of the reservoir temperature, as the geothermal reservoir is the surrounding rock mass in this case.

**Table 5:** Classification of geothermal resources by temperature.

| Resource | Muffler & Cataldi, (1978) | Hochstein, (1990**)** | Benderitter & Cormy, (1990**)** | Haenel, 1988, Dickson, (1990**)** |
|---|---|---|---|---|
| Low enthalpy | <90˚C | <125˚C | <100˚C | ≤150˚C |
| Intermediate enthalpy | 90-150˚C | 125-225˚C | 100-200˚C | --- |
| High enthalpy | >150˚C | >225˚C | >200˚C | >150˚C |

Temperature and enthalpy alone cannot define properly the state of geothermal fluids. Despite that fact, geothermal resources are classified as high-enthalpy fields (temperature is>150˚C), medium- enthalpy fields (temperature is 90˚C to 150 ˚C) and low-enthalpy fields (temperature is < 90˚C) according to their reservoir fluid temperatures (Muffler & Cataldi, 1978; Sanyal, 2010; Rybach, 2010). Based on the obtained values from geothermal temperature estimation, the reservoir temperature prediction can be carried out using the recent references (Williams, et al., 2011 and Younger, 2015) as shown in Tables 6, 7 and 8.

**Table 6:** The results of $Na^+$-$K^+$ cations geothermal classification

| No | Produced Water Wells | Geothermal Temperature Estimation (T ºC) | Reference: Williams, et al., 2011(see Figure 2) | Reference: Younger, 2015 (see Figure 1) |
|---|---|---|---|---|
| 1 | GialoW1 | 124.66 | Ultra low enthalpy | Medium enthalpy |
| 2 | GialoW2 | 138.67 | | |
| 3 | GialoW3 | 116.16 | | |
| 4 | GialoW4 | 121.44 | | |
| 5 | GialoW5 | 121.03 | | |
| 6 | GialoW6 | 124.34 | | |
| 7 | GialoW7 | 130.61 | | |
| 8 | GialoW8 | 128.99 | | |
| 9 | GialoW9 | 125.80 | | |
| 10 | GialoW10 | 123.27 | | |
| 11 | GialoW11 | 89.77 | | |
| 12 | GialoW12 | 101.91 | | |

**Table 7:** The results of $Na^+$-$K^+$-$Ca^{++}$ cations geothermal classification.

| No | Produced Water Wells | Geothermal Temperature Estimation (T ºC) | Reference | |
|---|---|---|---|---|
| | | | Williams, et al., 2011(see Figure 2) | Younger, 2015 (see Figure 1) |
| 1 | GialoW1 | 889.51 | High enthalpy | High enthalpy |
| 2 | GialoW2 | 956.34 | | |
| 3 | GialoW3 | 821.99 | | |
| 4 | GialoW4 | 847.54 | | |
| 5 | GialoW5 | 844.39 | | |
| 6 | GialoW6 | 886.15 | | |
| 7 | GialoW7 | 917.03 | | |
| 8 | GialoW8 | 902.76 | | |
| 9 | GialoW9 | 893.06 | | |
| 10 | GialoW10 | 882.26 | | |
| 11 | GialoW11 | 711.42 | | |
| 12 | GialoW12 | 772.48 | | |

**Table 8**: The results of $SiO_2$ geothermal classification.

| No | Produced Water Wells | Geothermal Temperature Estimation (T ºC) | Reference | |
|---|---|---|---|---|
| | | | Williams, et al., 2011(see Figure 2) | Younger, 2015 (see Figure1 ) |
| 1 | GialoW1 | 13.62 | Ultra low enthalpy | Very low enthalpy |
| 2 | GialoW2 | 19.21 | | |
| 3 | GialoW3 | 18.26 | | |
| 4 | GialoW4 | 17.69 | | |
| 5 | GialoW5 | 19.43 | | |
| 6 | GialoW6 | 22.96 | | |
| 7 | GialoW7 | 24.46 | | |
| 8 | GialoW8 | 22.51 | | |
| 9 | GialoW9 | 14.26 | | |
| 10 | GialoW10 | 12.10 | | |
| 11 | GialoW11 | 18.21 | | |
| 12 | GialoW12 | 11.20 | | |

**8. Conclusion**

Based on the results of calculations that have been done, the following conclusions could be drawn:

1. A large quantity of water were produced from oil wells.
2. These water exhibit a wide variation of their constituents and specifications.
3. The chemical constituents can be used as indicator for the prediction of geothermal temperatures.
4. It is possible to use the Na-K, Na-K-Ca and $SiO_2$ as geothermometer to estimate reservoir temperatures.
5. The $SiO_2$ geothermometer, display a low values of temperature comparing with the other two methods.
6. The geothermal classification of reservoirs according to the published references using enthalpy type revealed that there are a different enthalpies.
7. Based on the enthalpy categorization the geothermal of reservoir can be classified into Ultra low enthalpy, very low enthalpy, medium enthalpy and high enthalpy.
8. Consequently of these classification the potentiality of electric power generation varies according the geothermal temperature degree and the power plant system.
9. However, the geothermal temperature can be applied for direct and indirect geothermal applications.

**References**


[1] Ahmadi, A.; El Haj Assad, M.; Jamali, D.H.; Kumar, R.; Li, Z.X.; Salameh, T.; Al-Shabi, M.; Ehyaei, M.A. (2020) Applications of geothermal organic Rankine Cycle for electricity production. *J. Clean. Prod.* **2020**, *274*, 122950, DOI: 10.1016/j.jclepro.2020.122950.

[1] Aliyu, S.; Garba, M. M. (2019) Review on current global geothermal energy potentials and the future prospects. *Int. J. Adv. Sci. Eng.*, 5(4), DOI: 10.31695/ijasre.2019.33153.

[2] Avci, A. C.; Kaygusuz, O.; Kaygusuz, K. (2020) Geothermal energy for sustainable development. *J. Eng. Appl. Sci.*, *9* (1), 1414– 1426.

[3] Barbier, E. (2002) Geothermal energy technology and current status: an overview. *Renew. Sust. Energy Rev.*, *6* (1–2), 3– 65, DOI: 10.1016/S1364-0321(02)00002-3.
[4] Baujard, C.; Genter, A.; Cuenot, N.; Mouchot, J.; Maurer, V.; Hehn, R. (2018) Experience learnt from a successful soft stimulation and operational feedback after 2 years of geothermal power and heat production in Rittershoffen and Soultz-sous-Forêt plants (Alsace, France). *Geothermal Resource Council Reno.*, DOI: 10.5281/zenodo.3741736.
[5] https://chemport.cas.org/services/resolver?origin=ACS&resolution=options&coi=1%3ACAS%3A528%3ADC%252BB38XhtVSltrjF&md5=1ad7551674832c0c015e0e8a30512241
[6] DiPippo, R. (2012) Geothermal power plants: principles, applications, case studies and environmental impact. Butterworth-Heinemann.
[7] DiPippo, R.; Kitz, K. (2013) *Geothermal Binary Power Plants at Raft River, San Emidio, and Neal Hot Springs: Part 1—Plant Descriptions and Design Performance Comparison* , 2013; https://publications.mygeoenergynow.org/grc/1032225.pdf.
[8] Eyerer, S.; Schifflechner, C.; Hofbauer, S.; Bauer, W.; Wieland, C.; Spliethoff, H. (2021) Combined heat and power from hydrothermal geothermal resources in Germany: An assessment of the potential. *Renew. Sust. Energy Rev.*, *120*, 109661, DOI: 10.1016/j.rser.2019.109661
[9] Feng, R.; Balling, N.; Grana, D. (2020) Lithofacies classification of a geothermal reservoir in Denmark and its facies-dependent porosity estimation from seismic inversion. *Geothermics*, *87*, 101854, DOI: 10.1016/j.geothermics.2020.101854
[10] Frick, S.; Kranz, S.; Kupfermann, G.; Saadat, A.; Huenges, E. (2019) Making use of geothermal brine in Indonesia: binary demonstration power plant Lahendong/Pangolombian. *Geotherm. Energy*, *7* (1), 30, DOI: 10.1186/s40517-019-0147-2
[11] Giggenbach, W. F. (1988) "Geothermal solute equilibria. derivation of Na-K-Mg-Ca geoindicators," Geochim. Cosmochim. Acta, vol. 52, no. 12, pp. 2749–2765.
[12] Holdmann, G. (2007) The Chena Hot Springs 400kW geothermal power plant: experience gained during the first year of operation. *Trans. - Geotherm. Resour. Counc.*, *31*, 515– 519
[13] Idroes R. *et al.*, (2019) "Geochemistry of warm springs in the Ie Brôuk hydrothermal areas at Aceh Besar district," in *IOP Conference Series: Materials Science and Engineering*, vol. 523, no. 1, p. 12010.
[14] IEA. World Energy Outlook 2020 , (2020); https://www.iea.org/reports/world-energy-outlook-2020
[15] Ikshvaku, V.; Sharma, S.; Maurya, V.; Saroj, A. (2018) Geothermal Energy: An Effective Means of Renewable Energy Source. *International Research Journal of Engineering and Technology (IRJET)*, *5* (10), 389
[16] Kabeyi, M. J. B. (2019) Geothermal electricity generation, challenges, opportunities and recommendations. *Int. J. Adv. Sci. Res. Eng.*, *5* (8), 53– 95, DOI: 10.31695/IJASRE.2019.33408
[17] Legmann, H. (2003) The Bad Blumau geothermal project: a low temperature, sustainable and environmentally benign power plant. *Geothermics*, *32* (4–6), 497– 503, DOI: 10.1016/S0375-6505(03)00067-1
[18] Mahmoudi, A.; Fazli, M.; Morad, M. R. (2018) A recent review of waste heat recovery by Organic Rankine Cycle. *Appl. Therm. Eng.*, *143*, 660– 675, DOI: 10.1016/j.applthermaleng.2018.07.136
[19] Maryanto, S., et al., (2017) "Magnetotelluric geochemistry investigations of blawan geothermal field, East Java, Indonesia," Geosciences, vol. 7, no. 2, p. 41.
[20] Milliken, M. (2017) Geothermal resources at Naval petroleum reserve-3 (NPR-3), Wyoming. *Proceedings of 32nd Workshop on Geothermal Reservoir Engineering* , Stanford University, Stanford, CA.
**[21]** Muffler, P., & Cataldi, R. (1978). Methods for regional assessment of geothermal resources. Geothermics.
[22] Morgan, P. (1984) The thermal structure and thermal evolution of the continental lithosphere. *Phys. Chem. Earth.*, *15*, 107– 193, DOI: 10.1016/0079-1946(84)90006-5
[23] Nelson, D. (2017) Geothermal Energy: Pros and Cons. *Sci. Trends*, 132
[24] Pernecker, G.; Uhlig, S. (2002) Low enthalpy power generation with ORC-Turbogenerator The Altheim Project, Upper Austria. *GHC Bulletin.*, *23* (1), 26– 30
[25] Rybach, L. (2010). Legal and regulatory environment favourable for geothermal development investors. In: *Proceedings World Geothermal Congress 2010*, Bali, Indonesia, 25-30 April 2010. Available at: www.geothermal-energy.org/pdf/ IGAstandard/WGC/2010/0303.pdf.
[26] Santamaria, M. E. (2020) *Geothermal Energy*.
[27] Sanyal, S.K. (2010). On minimizing the levelized cost of electric power from Enhanced Geothermal Systems. In: *Proceedings World Geothermal Congress2010*, Bali, Indonesia, 25-30 April 2010. Available at: www.geothermal- energy. org/pdf/IGAstandard/WGC/2010/3154.pdf.
[28] Shmeleva, M. (2018) *Geothermal Energy Production from Oil and Gas Wells*; http://www.diva-portal.org/smash/get/diva2:1293872/FULLTEXT01.pdf

[29] Tchanche, B. F.; Loonis, P.; Pétrissans, M.; Ramenah, H. (2013) Organic Rankine cycle systems Principles, opportunities and challenges. *25th International Conference on Microelectronics (ICM)*; pp. 1– 4.
[30] Veil JA, Puder MG, Elcock D, Redweik Jr RJ. (2004) A white paper describing produced water from production of crude oil, natural gas and coal bed methane. Argonne National Laboratory, Prepared for US Department of Energy, National Energy Technology Laboratory Under Contract W-31-109-Eng-38.
[31] Watanabe, N.; Blöcher, G.; Cacace, M.; Held, S.; Kohl, T. (2017) Case Study: Soultz-sous-Forêts. *Geoenergy Modeling III*; Springer, 2017; pp. 75– 93.
[32] Williams, C. F.; Reed, M. J.; Anderson, A. F. (2011) Updating the classification of geothermal resources. *Proceedings Thirty-Sixth Workshop on Geothermal Reservoir Engineering*.
[33] Younger, P.L. (2015). Geothermal Energy: Delivering on the Global Potential. Basel: MDPI AG.